



This is an open access article distributed under the terms of the Creative Commons Attribution 4.0 International License (CC BY 4.0), which permits use, distribution, and reproduction in any medium, provided the original publication is properly cited. No use, distribution or reproduction is permitted which does not comply with these terms.

SHAPE OPTIMIZATION OF A COLUMN MODELLING THE BRIDGE SPAN UNDER A SPECIFIC LOAD - NUMERICAL AND EXPERIMENTAL STUDIES

Janusz Szmidla, Anna Jurczyńska*

Czestochowa University of Technology, Czestochowa, Poland

*E-mail of corresponding author: anna.jurczynska@pcz.pl

Janusz Szmidla 0000-0002-7475-7925,

Anna Jurczyńska 0000-0002-8505-3157

Resume

This work is dedicated to the problem of optimizing the shape of columns modelling bridge span subjected to the selected specific load case. Based on Hamilton's principle, motion equations and boundary conditions were defined. Taking into account the static criterion of loss of stability and the condition of constant volume of systems, the values of geometric parameters of the analyzed column were determined at which the maximum critical load value was obtained. The simulated annealing algorithm was used to find the maximum critical force being a function of many variables. Within the kinetic criterion of loss of stability, the range of changes in the natural frequency of optimized columns as a function of external load was determined. Based on the obtained results it was concluded that it is possible to control the dynamic properties while improving the stability of the system.

Article info

Received 1 March 2023

Accepted 18 June 2023

Online 10 July 2023

Keywords:

bridge span
shape optimization
nonprismatic rod
free vibrations
stability

Available online: <https://doi.org/10.26552/com.C.2023.059>

ISSN 1335-4205 (print version)

ISSN 2585-7878 (online version)

1 Introduction

The issue of stability and free vibrations plays a significant role in the design and exploitation of mechanical devices and civil engineering structures. With proper system operation, correctly conducted static and dynamic analyzes guarantee that the machine or structure will not be damaged at stresses much lower than the allowable one. Currently, scientists' research is focused on increasing the strength of structures and the possibility of controlling their dynamic properties. Among the factors that are analyzed in the context of improving the properties of slender systems - devices or their parts are, among others:

- the possibility of using elastic or piezoceramic elements, supporting the systems with elastic foundations with different characteristics [1-6] or using oscillators [7];
 - analysis of nonlinearities in the system: geometric [7-11], material (physical) [8, 12-14], resulting from friction [8];
 - optimization of the shape of the system [15-17].
- The last two factors are of a particular importance.

Changing the shape of the structural elements can affect not only the strength, but it can also reduce the weight of the structure and thus lower the costs. Including nonlinearities in the models increases the quality of mapping the actual behaviour of the system - it enables a more accurate study of the behaviour of the system during operation. The role of stability and vibrations of slender systems has received increased attention in recent years, across a number of disciplines. Physical models, similar to those analyzed in this paper, are commonly found in constructions (bridge spans) [18-23] or in the mining industry (support structures).

A new approach to the stability studies of non-prismatic Bernoulli-Euler columns loaded axially was proposed in [16]. The described method of rigid elements consists of dividing a column into n segments, then each of them is additionally divided into k members. Each of the segments from the first division can be replaced with a rigid, multi-segment joint element (two rigid segments connected by a joint and springs: translational and rotating). The research considered double symmetrical columns with a cross-section that change continuously and stepwise (multi-segment system).

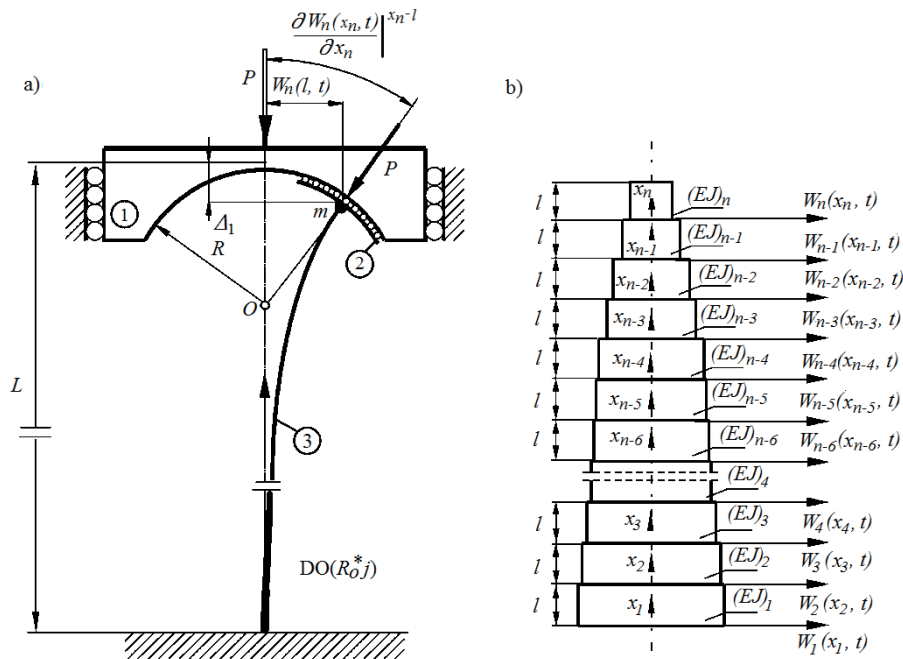


Figure 1 Physical model of the column a) under follower force directed towards positive pole, b) division into segments

The problem of stability was also dealt with by Li [24-25]. In his works, he analyzed columns with a stepped and continuous change of the cross-section along the axis. The research covered the impact of various load cases (conservative or tracking), system geometry and mounting methods, including support by rotational and translational springs, on the value of the critical load. The transfer matrix method and the finite element method were used to solve the boundary problems presented in the works.

An explicit equation for the buckling load value of the non-prismatic columns with non-uniform distribution of longitudinal forces was developed in [26]. Taking into account the Euler dependence on the critical load, the authors presented a series of graphs specifying the value of the correction factor taking into account the type of convergence, the size of the cross-section and the method of loading the structure. The maximum recorded error, resulting from the comparison of the proposed method and analytical calculations, did not exceed 7%.

This article deals with the issue of stability and free vibrations of a geometrically nonlinear column with a nonprismatic element, modelling the bridge support structure. The analysis covered the change of the bifurcation load (only the loss of the rectilinear form of the static equilibrium was examined) and the change of the natural frequency. The shape of the bar with a variable cross-section was optimized using a modified simulated annealing algorithm. The theoretical and numerical studies were experimentally verified.

2 Physical model of the system

Figure 1 presents a physical model of the considered column in the construction variant of loading heads 1 and load taking heads 2 with a circular outline (constant curvature). Under the follower load, with the force directed towards the positive pole (case of specific load), the direction of the loading force goes through the fixed point O - the centre of the loading and load taking head. The parts of the load taking heads are infinitely rigid. The columns 3 are rigidly fixed on one side ($x_1 = 0$) and they are connected at the free end ($x_n = l$) with the load taking head 2. Reduced mass of elements, being a part of the load taking head was taken into account in the field with the point mass m .

The method of issue description adopted in this paper consists in the division of a column (Figure 1b) into smaller segments (with indexes $I = 1..n$) with a circular cross-section, mass per unit length (ρA_i) and flexural rigidity (EJ_i), described by length l and diameter d , as well as the transverse displacement $W_i(x_i, t)$. The optimization of the shape is limited to selection of diameters of particular segments of the systems at which the maximum critical load value is obtained. This assumption causes that the maximum value of critical force, which is a function of many variables (diameters and lengths of particular column segments) is searched for:

$$P_{\max} = f\left(d_1, d_2, \dots, d_n, \frac{L}{n}\right). \quad (1)$$

The value of the critical force P_{kr} of the optimized columns was related to the constant along the length L of the flexural rigidity $(EJ)_{pr}$ of comparison columns:

$$\lambda_{oc} = \frac{P_{kr} L^2}{(EJ)_{pr}}. \quad (2)$$

In the solution of the subject issue, the constant total length L , the constant total volume V , constant value of the longitudinal elasticity E , as well as optimized and relevant comparison (prismatic) columns, are assumed.

In this section, exemplary designations of the considered columns have been implemented:

- $DO(R^*)$ - optimized column subjected to the follower force load, directed towards the positive pole with a stepwise variable flexural rigidity, with the parameter of the loading and load taking head R^* ;
- $DP(R^*)$ - the column with a constant at the length of the flexural rigidity system $(EJ)_{pr}$ (comparative) subjected to load with tracking force directed towards the positive pole, with the parameter of the loading head R^* .

3 Equations of the boundary problem

Determination of motion equations and boundary conditions of the considered systems was conducted under the Hamilton's principle (the principle of least action):

$$\delta \int_{t_1}^{t_2} \left(T - \sum_{\xi=1}^3 V_{\xi} \right) dt = 0, \quad (3)$$

Where T means kinetic energy, V - potential energy, t - time, δ - operator of variations.

The kinetic energy T of the considered columns is the sum of the kinetic energy of the column and kinetic energy of the body of mass m (transverse inertia):

$$T = \sum_{i=1}^n \frac{(\rho A_i)}{2} \int_0^l \left[\frac{\partial W_i(x_i, t)}{\partial t} \right]^2 dx_i + \frac{m}{2} \left[\frac{\partial W_n(l, t)}{\partial t} \right]^2, \quad (4)$$

where A_i - is the cross-sectional area of the i -th segment of the optimized column.

The components of the potential energy were defined as follows:

- flexural elastic energy:

$$V_1 = \sum_{i=1}^n \frac{(EJ_i)}{2} \int_0^l \left[\frac{\partial^2 W_i(x_i, t)}{\partial x_i^2} \right]^2 dx_i, \quad (5)$$

- energy of the force P vertical component:

$$V_2 = -\frac{P}{2} \sum_{i=1}^n \int_0^l \left[\frac{\partial W_i(x_i, t)}{\partial x_i} \right]^2 dx_i, \quad (6)$$

- energy of the force P horizontal component:

$$V_3 = \frac{P}{2} R \left[\frac{\partial W_n(x_n, t)}{\partial x_n} \right]_{x_n=1}^2, \quad (7)$$

where:

$$\varphi = \frac{W_0}{R-r} = \frac{R \frac{\delta W_n(x_n, t)}{\delta x_n} \Big|_{x_n=l} - W_n(l, t)}{R-r}, \quad (8)$$

$$\beta_0 = \frac{W_n(l, t) - r \frac{\delta W_n(x_n, t)}{\delta x_n} \Big|_{x_n=l}}{R-r}.$$

Known a priori, the geometrical boundary conditions of the considered problem, are:

- at the attachment point ($x_1 = 0$):

$$W_1(0, t) = \frac{\partial W_1(x_1, t)}{\partial x_1} \Big|_{x_1=0} = 0, \quad (9)$$

- continuity conditions

$$W_{\zeta}(l, t) = W_{\zeta+1}(0, t), \frac{\partial W_{\zeta}(x_{\zeta}, t)}{\partial x_{\zeta}} \Big|_{x_{\zeta}=1} = \frac{\partial W_{\zeta+1}(x_{\zeta+1}, t)}{\partial x_{\zeta+1}} \Big|_{x_{\zeta+1}=0}, \text{ where } \zeta = 1 \dots (n-1). \quad (10)$$

After application of geometrical dependencies between the elements of the head taking the load, with the follower force directed towards the pole, the following was obtained:

$$W_n(l, t) - R \frac{\partial W_n(x_n, t)}{\partial x_n} \Big|_{x_n=l} = 0. \quad (11)$$

Considering the Hamilton's principle in Equation (3), after a priori application of the relevant boundary conditions in Equations (9)-(11) and after algebraic transformations, it was obtained:

- differential equations of motion of the considered system:

$$(EJ_i) \frac{\partial^4 W_i(x_i, t)}{\partial x_i^4} + P \frac{\partial^2 W_i(x_i, t)}{\partial x_i^2} + (\rho A_i) \frac{\partial^2 W_i(x_i, t)}{\partial t^2} = 0, i = 1 \dots n, \quad (12)$$

- natural continuity conditions:

$$\frac{\partial^2 W_{\zeta}(x_{\zeta}, t)}{\partial x_{\zeta}^2} \Big|_{x_{\zeta}=1} = \frac{\partial^2 W_{\zeta+1}(x_{\zeta+1}, t)}{\partial x_{\zeta+1}^2} \Big|_{x_{\zeta+1}=0}, \quad (13)$$

$$\frac{\partial^3 W_\zeta(x_\zeta, t)}{\partial x_\zeta^3} \Big|_{x_\zeta=1} = \chi_{\zeta+1} \frac{\partial^3 W_{\zeta+1}(x_{\zeta+1}, t)}{\partial x_{\zeta+1}^3} \Big|_{x_{\zeta+1}=0}, \quad (14)$$

- natural boundary conditions at the free end of the systems ($x_n = l$):

$$\frac{\partial^2 W_n(x_n, t)}{\partial x_n^2} \Big|_{x_n=1} - \frac{1}{R} \frac{\partial^2 W_n(x_n, t)}{\partial x_n^2} \Big|_{x_n=1} - \frac{m}{(EJ_n)} \frac{\partial^2 W_n(x_n, t)}{\partial t^2} = 0, \quad (15)$$

where: $k_n^2 = P/(EJ_n)$, $\chi_{\zeta+1} = (EJ_{\zeta+1})/(EJ_\zeta)$.

4 Solution of the boundary problem - energetic method

Conducting research on optimization requires knowledge of the critical load values of the considered columns, with the adopted criterion of constant volume. To determine the critical load parameter, it is sufficient to apply the static stability criterion (energetic method). Condition for the existence of a minimum total potential energy was recorded in the following form:

$$\partial \sum_{\xi=1}^3 V_\xi = 0. \quad (16)$$

Potential energy of the system (see Equations (5)-(7)), after previous separation of variables of the function $W_i(x_i, t)$, in relation to spatial x_i and time t coordinates:

$$W_i(x_i, t) = y_i(x_i) \cos(\omega t), \quad (17)$$

has the following form:

$$\sum_{\xi=1}^3 V_\xi = \sum_{i=1}^n \frac{(EJ_i)}{2} \int_0^l [y_i''(x_i)]^2 dx_i - \frac{P}{2} \sum_{i=1}^n \int_0^l [y_i'(x_i)]^2 dx_i + \frac{PR}{2} [y_i'(l)]^2. \quad (18)$$

The boundary conditions in Equations (9)-(11), (13)-(15) after applying Equation (17) are as follows:

$$y_1(0) = y_1'(0) = 0, \quad (19)$$

$$y_n(l) = Ry_n'(l), \quad (20)$$

$$y_n'''(l) - \frac{1}{R} y_n''(l) = 0, \quad (21)$$

$$y_\zeta(l) = y_{\zeta+1}(0), \quad (22)$$

$$y_\zeta'(l) = y_{\zeta+1}'(0), \quad (23)$$

$$y_\zeta''(l) = \chi_{\zeta+1} y_{\zeta+1}''(0), \quad (24)$$

$$y_\zeta'''(l) = \chi_{\zeta+1} y_{\zeta+1}'''(0). \quad (25)$$

Taking into account the Equations (18), (19) and (22) - (24) in Equation (16), the following displacement equations were obtained:

$$y_i^{IV}(x_i) + k_i^2 y_i''(x_i) = 0, \quad i = 1 \dots n. \quad (26)$$

The general solutions of Equation (26) were described by the function:

$$y_i(x_i) = D_{i1} \sin(k_i x_i) + D_{i2} \cos(k_i x_i) + D_{i3} x_i + D_{i4}, \quad (27)$$

where D_{ik} are integration constants ($k = 1, \dots, 4$).

Based on the solutions of Equation (27) of displacement equations and relevant boundary conditions in Equations (19)-(25), a system of equations was obtained, which in the matrix form, was recorded as follows:

$$G_s \Lambda = 0 \quad (28)$$

where: $\Lambda = [D_{11} \ D_{11} \ D_{11} \ D_{11} \ \dots \ D_{n1} \ D_{n2} \ D_{n3} \ D_{n4}]^T$ and G_s means the square matrix of a degree dependent on the number of n segments of considered columns.

Thus, the following is obtained:

$$G_s = \begin{bmatrix} F_0 & 0 & 0 & 0 & 0 & 0 & 0 \\ H_1^0 & H_2^0 & 0 & 0 & 0 & 0 & 0 \\ 0 & H_2^0 & H_3^0 & 0 & 0 & 0 & 0 \\ 0 & 0 & 0 & H_{n-2}^0 & H_{n-1}^0 & 0 & 0 \\ 0 & 0 & 0 & 0 & H_{n-1}^0 & H_n^0 & 0 \\ 0 & 0 & 0 & 0 & 0 & F_n & 0 \end{bmatrix}, \quad (29)$$

$$F_0 = \begin{bmatrix} 0 & 1 & 0 & 1 \\ k_1 & 0 & 1 & 0 \end{bmatrix}$$

$$H_{\zeta+1}^0 = \begin{bmatrix} 0 & -1 & 0 & -1 \\ -k_{\zeta+1} & 0 & -1 & 0 \\ 0 & \chi_{\zeta+1} k_{\zeta+1}^2 & 0 & 0 \\ \chi_{\zeta+1} k_{\zeta+1}^3 & 0 & 0 & 0 \end{bmatrix},$$

$$H_\zeta^1 = \begin{bmatrix} \sin(k_\zeta l) & \cos(k_\zeta l) & l & 1 \\ k_\zeta \cos(k_\zeta l) & -k_\zeta \sin(k_\zeta l) & 1 & 0 \\ -k_\zeta^2 \sin(k_\zeta l) & -k_\zeta^2 \cos(k_\zeta l) & 0 & 0 \\ -k_\zeta^3 \cos(k_\zeta l) & k_\zeta^3 \sin(k_\zeta l) & 0 & 0 \end{bmatrix}, \quad (30)$$

$$F_n = \begin{bmatrix} f_{11} & f_{12} & f_{13} & f_{14} \\ f_{21} & f_{22} & f_{23} & f_{24} \end{bmatrix}.$$

The matrix coefficient F_n was recorded as:

$$f_{11} = -k_n^3 \cos(k_n l) + \frac{k_n^2 \sin(k_n l)}{R},$$

$$f_{12} = k_n^3 \sin(k_n l) + \frac{k_n^2 \cos(k_n l)}{R}, f_{13} = 0, f_{14} = 0, \quad (31)$$

$$f_{21} = \sin(k_n l) - R k_n \cos(k_n l),$$

$$f_{22} = \cos(k_n l) + R k_n \sin(k_n l), f_{23} = l - R, f_{24} = 1.$$

The transcendental equation for the critical load value is as follows:

$$\det G_s = 0.$$

(32)

$$\begin{aligned} \alpha_i^2 &= \sqrt{-0.5k_i^2 + (0.25k_i^4 + \Omega_i^2)}, \\ \beta_i^2 &= \sqrt{-0.5k_i^2 + (0.25k_i^4 + \Omega_i^2)}, \\ \Omega_i^2 &= \frac{(\rho A_i)\omega^2}{(EJ_i)}, \quad k_i = \sqrt{\frac{P}{(EJ_i)}}. \end{aligned} \quad (35)$$

5 Solution of the boundary issue - vibration method

Based on the solution of the boundary issue with the kinetic criterion of stability, the range of changes in natural vibrations frequency ω as a function of the external load P of the considered columns was determined. For this purpose, Equations of motion (12) are taken into account, which, after separating the variables with respect to spatial coordinates x_i and time t (see the Equation (17)), are in the following form:

$$y_i^{IV}(x_i) + k_i^2 y_i''(x_i) - \Omega_i^2 y_i(x_i) = 0, \quad i = 1 \dots n. \quad (33)$$

The results of Equations (33) are:

$$y_i(x_i) = C_{1i} \cosh(\alpha_i x_i) + C_{2i} \cos(\beta_i x_i) + C_{3i} \sinh(\alpha_i x_i) + C_{4i} \sin(\beta_i x_i), \quad (34)$$

where C_{ki} are integration constants ($k = 1, \dots, 4$) and:

After applying Equation (34) to relevant boundary conditions, the following system of equations was obtained:

$$G_D \text{col}\{C_{11} \ C_{21} \ C_{31} \ C_{41} \ \dots \ C_{1n} \ C_{2n} \ C_{3n} \ C_{4n}\} = 0. \quad (36)$$

The determinant of the matrix of coefficients G_D equalized to zero is a transcendental equation on the neutral vibrations frequency ω (within the range of loss of the rectilinear form of the static equilibrium) of the considered systems, that is:

$$G_D \text{col}\{C_{11} \ C_{21} \ C_{31} \ C_{41} \ \dots \ C_{1n} \ C_{2n} \ C_{3n} \ C_{4n}\} = 0. \quad (37)$$

6 Simulated annealing

The method of simulated annealing consists in a heuristic algorithm belonging to the class of non-

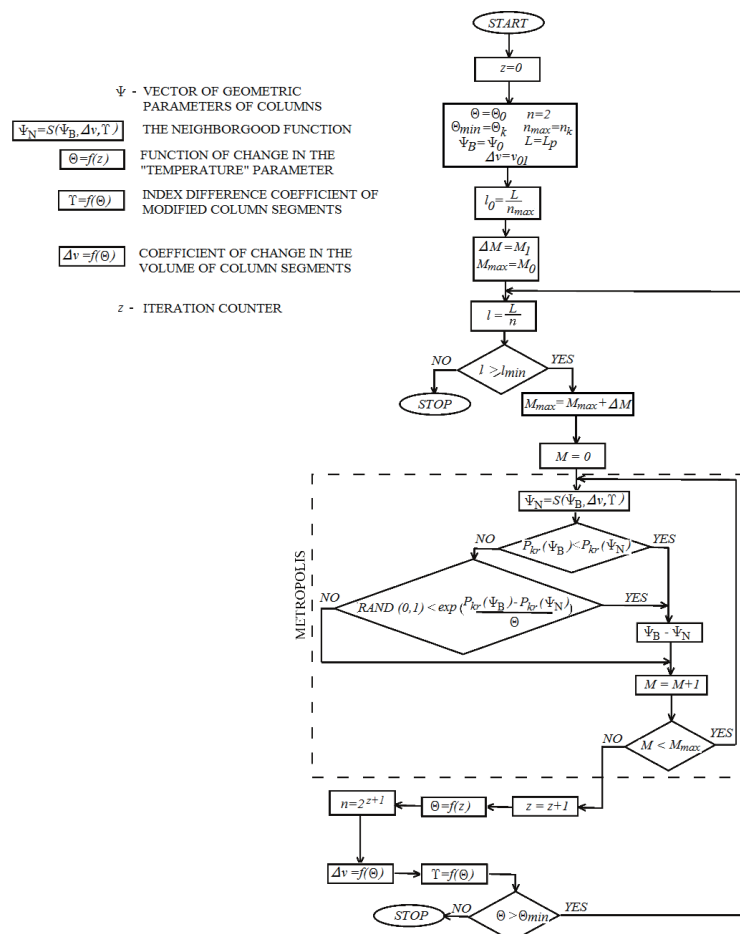


Figure 2 A block diagram of the modified method of simulated annealing

deterministic algorithms. This method is a modification of the “hill climbing algorithm”. The performance of the algorithm requires defining four parameters: the initial representation of the result, the generator of random changes in the results (neighbourhood function), the evaluation function (cost) and the annealing schedule. The additional parameter Θ called “temperature” is not directly related to variables subjected to optimization, but it only controls the performance of the algorithm. The value of the parameter Θ affects only the probability of passing from one point in the search space to another and is selected in a manner depending on a given optimization issue.

Figure 2 presents a block diagram of the applied method of simulated annealing. In the considered method, a new solution Ψ_N selected by modifying the current result Ψ_B , is always accepted when an increase is obtained in the value of the function of the result evaluation defined by Equation (1). Otherwise, the acceptance occurs with a certain probability equal to:

$$p_a = \exp\left(-\frac{\Delta f}{\Theta}\right), \quad (38)$$

where: Δf is the difference of the value of the evaluation function defined by the Equation (1) and:

$$\Psi = \left[d_1 \ d_2 \ \dots \ d_{n-2} \ d_{n-1} \ d_n \ \frac{L}{n} \right]. \quad (39)$$

The core of the algorithm is the procedure called Metropolis, which was used for simulation of the annealing process under a given “temperature” Θ . In the Metropolis procedure, a number of iterations defined by the parameter M was performed at the same value of the parameter Θ . Then, the “temperature” was reduced according to the adopted “annealing schedule”, which was described by the dependency $\Theta = f(z)$ (see Figure 3a). The number of M_{\max} iterations in subsequent initiation of the Metropolis procedure was increased by a certain value ΔM .

7 Modified method of simulated annealing

In the method of simulated annealing, apart from the change of the value of parameters Θ and M , an additional modification of the performance of the function $S(\Psi_B)$ was assumed, which generates a neighbourhood result (neighbourhood function). In the considered case, the performance of the neighbourhood function was changed along with the change of the “temperature” parameter (Figure 3).

The applied method of selection of a new shape consists in the “transfer” of a certain part of volume, described by the coefficient Δv , from a randomly selected segment (with the index i) to another segment of the column (with the index j), selected also in a random manner (Figure 3b). This is done by changing the diameters of selected segments (d_i, d_j) into new diameters (d'_i, d'_j). The lengths of segments l remain unchanged. Thanks to application of such a solution, the fixed column volume criterion, adopted in this paper, has been met. New diameters of segments are calculated from the equations:

$$d'_i = \sqrt{(1 - \Delta v)d_i}, \quad d'_j = \sqrt{d_j + \Delta v d_i}, \quad (40)$$

where: $i, j \in (0..n)$ - indices of the segments subjected to modifications, $\Delta v \in (0..1)$ - volume change coefficient.

The maximum allowable difference between indices of segments $|i - j|$, the diameters of which (d_i, d_j) are changed and the volume change factor Δv ($\Delta v = f(\Theta)$), defining what part of the volume of a given segment (with the index i) will be transferred to another segment (with the index j), are also changed. The segment whose volume is increased (diameter d'_j) is any segment of the column selected in a random manner. The segment described by the parameter of the diameter d'_i , the volume of which is reduced, is also selected in a random manner, however, in this case some restrictions are imposed on the selection.

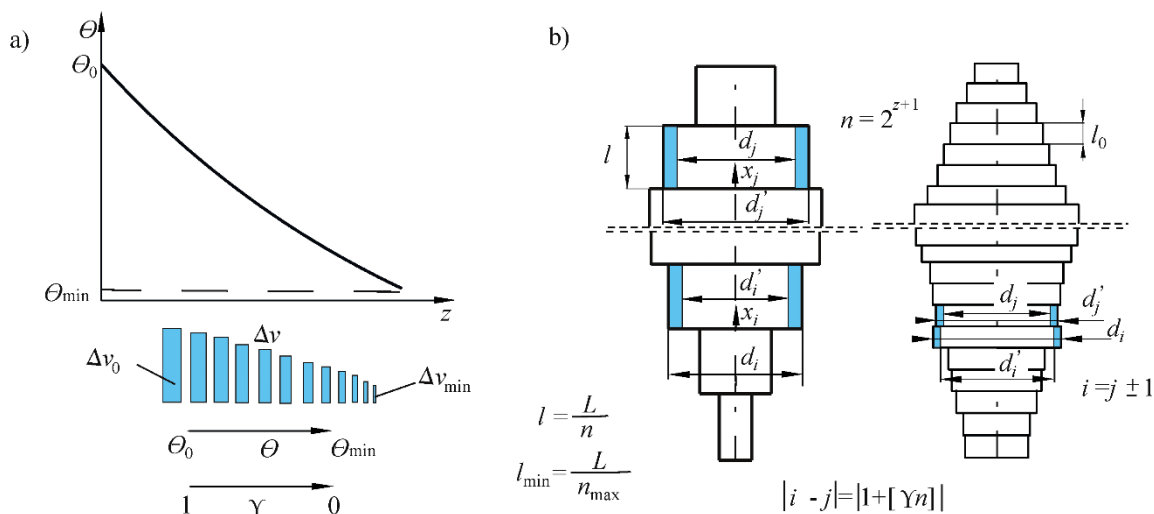


Figure 3 a) change of the “temperature” parameter, b) modification of the neighbourhood function

At the initial stage of optimization, selection of this segment can be completely random. However, at the final stage, it is possible to select only one of the two segments adjacent to the element whose volume is increased ($i = j \pm 1$). The maximum difference of indices of modified segments, defined as the product of the number of segments n and the coefficient Y ($Y = f(\Theta)$), where $Y=1...0$. Taking into account the second variable parameter, the volume change coefficient Δv , a certain set value of Δv_0 was assumed at the beginning of the calculation. Those values were decreased together with the decrease of the parameter, until the minimum value Δv_{\min} , defined at the beginning, was reached at Θ_{\min} (Figure 3). The application of such a solution significantly accelerated the optimization process, especially at the beginning of the calculation. The parameters Δv , Y , similar to Θ and M were modified after each time the Metropolis procedure was carried out. As a result of the described modification, the neighbourhood function was recorded as:

$$\Psi_N = S(\Psi_B, \Delta v, Y). \quad (41)$$

Another implemented modification of the algorithm of simulated annealing is a change of the number of segments n constituting a part of a slender system, made together with the change in the value of the mentioned parameters, that is:

$$n = 2^{z+1}. \quad (42)$$

Each segment of the column is divided into two segments with lengths equal to half of the length of the divided segment. The diameters of both segments are equal to the diameter of the divided segment. In the considered cases of column loads, the system was originally divided into two segments ($z = 0$). The number of segments n into which the slender system was divided, was changed in geometrical progression with a quotient equal to 2 to n_{\max} value (maximum number of segments). The division was carried out after each Metropolis step loop until the length of the segment l was greater or equal to the minimum length l_{\min} :

$$l_{\min} = \frac{L}{n_{\max}}. \quad (43)$$

Implementation of the above-mentioned modifications to the algorithm of simulated annealing results in a significant acceleration of the shape optimization process. Thanks to the initial division into a small number of segments, it is possible to quickly determine the “coarse” shape of the columns. At the final stage of calculations, when the length of segments is short, small changes in shape result in smoothing the shape of the systems.

7.1 Function of changing the “temperature” parameter

A significant problem in the simulated annealing is the appropriate selection of the method of lowering the parameter Θ . Too rapid lowering of the “temperature” has a negative effect on the accuracy of the algorithm, too slow - increases the calculation time. The parameter Θ is used in determining the probability of acceptance (see Equation (34)) of the worse solution. This probability depends on the difference in the evaluation function Δf , as well. The application of variable parameters of neighbourhood generation and the change in the number of segments n of the system causes that the mean value Δf decreases with each implementation of Metropolis. In the analyzed cases, the mean value Δf had almost exactly double in each successive Metropolis. The described change should be taken into account in the “annealing schedule”. For the statement $(-\Delta f / \Theta)$ in Equation (34) to behave as expected, the value of the parameter Θ should be reduced accordingly in each iteration z .

8 The results of numerical calculations and experimental research

This section presents the results of numerical calculations with the use of a static and kinetic stability criterion. In the considered case of a specific load, appropriate results of theoretical research were presented, with selected geometrical parameter of the load taking heads, that is R_o^* .

Based on the energy method, the scope of critical load changes of optimized columns and their shape was determined, with the assumed criteria of the fixed volume of the systems. The scope of changes in the natural vibrations in the external load function and the form of vibrations were obtained by solving the boundary conditions, using the vibration method. Additional experimental research was carried out with regard to the value of natural vibrations frequency.

8.1 Results of numerical calculations - static stability criterion

Taking into consideration the transcendental equation for the value of critical value (see the Equation (32)), numerical calculations were carried out to determine the maximum value of the critical force P_{kr} of columns, in the considered cases of natural load. Numerical calculations were carried out dividing the column into $n = 128$ segments. The introduction of the division of columns into a larger amount of segments did not significantly affect the obtained result and

it extended the time of numerical calculations. The obtained increase in the critical load with division into 128 and 256 segments differed by at most 0.18%. The value of critical load of optimized system $DO(R_o^* j)$ and the parameters of load taking heads were related to the total constant length L of the system and the constant flexural rigidity $(EJ)_p$ of prismatic (comparative) column $DP(R_o^* j)$.

Figure 4 shows the scope of changes in the critical parameters of the column load as a function of changes in the parameters of load taking heads. The results of numerical calculations were presented in the case of the systems with an optimized shape $DO(R_o^* j)$ (solid lines) and corresponding columns $DP(R_o^* j)$ (dashed lines) with a constant along the length of the flexural rigidity system.

At the considered values of the radius R of the loading head, each of the critical load change curves was characterized by occurrence of the maximum value of the critical load parameter λ_{oc} . In the case of comparative columns with fixed flexural rigidity $(EJ)_p$ the extreme value is determined at parameters $R_o^* = 0.5$. The range of the value of radius R of the loading head, changing from zero to the length of the column $L(R_o^* \in \langle 0, 1 \rangle)$ was taken into account in the calculation. If $R_o^* = 0$, then the Euler's load case is obtained.

The percentage increase in the critical load δ_o of the

optimized column with the changed flexural rigidity is presented in Figure 5, where:

$$\delta_o = \frac{\lambda_{ocDO}(R_o^* j) - \lambda_{ocDP}(R_o^* j)}{\lambda_{ocDP}(R_o^* j)} 100\% \quad (44)$$

Considering the division of columns into $n = 128$ segments, the critical load increase by at most 40.64% was obtained.

Figure 6 shows the shapes of models of optimized columns (optimum diameter distribution), with selected geometrical parameters of loading and load taking heads. The physical models of considered columns (see Figure 1) were built from segments which have been described by a fixed diameter d_i and fixed length l .

As a result of numerical calculations of the optimization issue, "stepped" shapes of the systems were obtained. Due to a significant number of segments, in relation to the total length L of columns, the actual shapes were approximated by polynomials of a relevant degree (with the highest possible correlation coefficient and the lowest standard deviation, in relation to the actual shapes) and they were drawn as smooth. Taking into account the assumed criterion for the constant volume of systems, the outline of prismatic (comparative) columns are marked with the dashed lines. For each of the presented shapes, values of the critical force, the

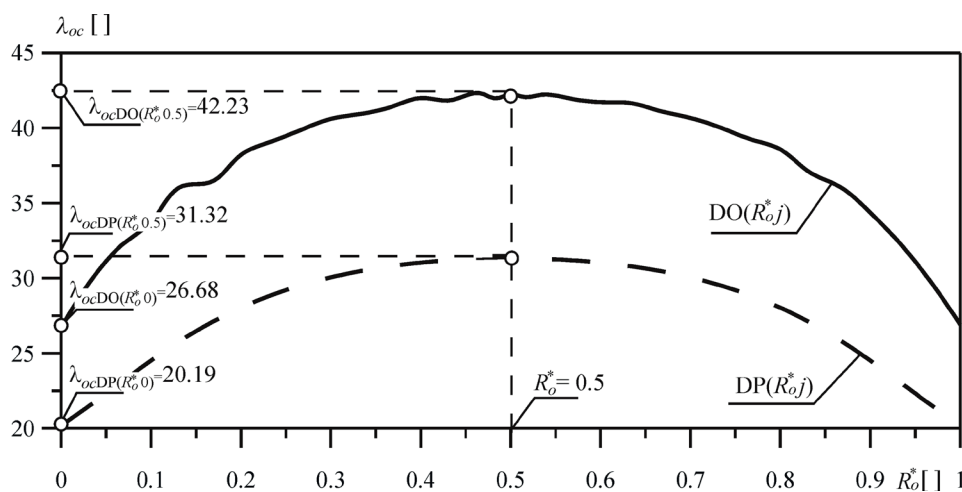


Figure 4 Change of the critical load parameter λ_{oc} as a function of the parameter value R_o^* of columns $DO(R_o^* j)$, $DP(R_o^* j)$

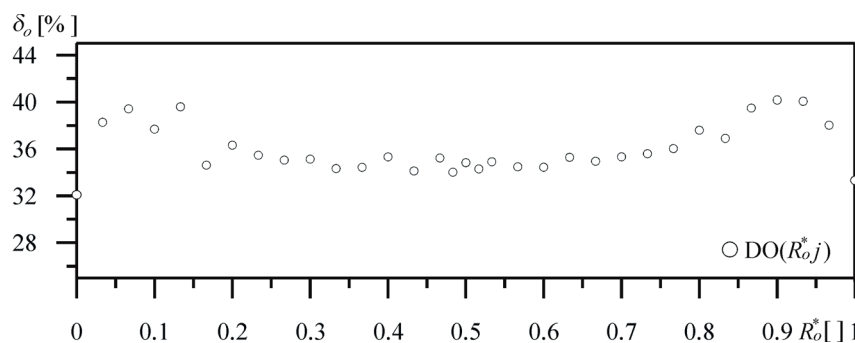


Figure 5 The percentage increase in the critical load δ_o as a function of the parameter value R_o^* of columns $DO(R_o^* j)$

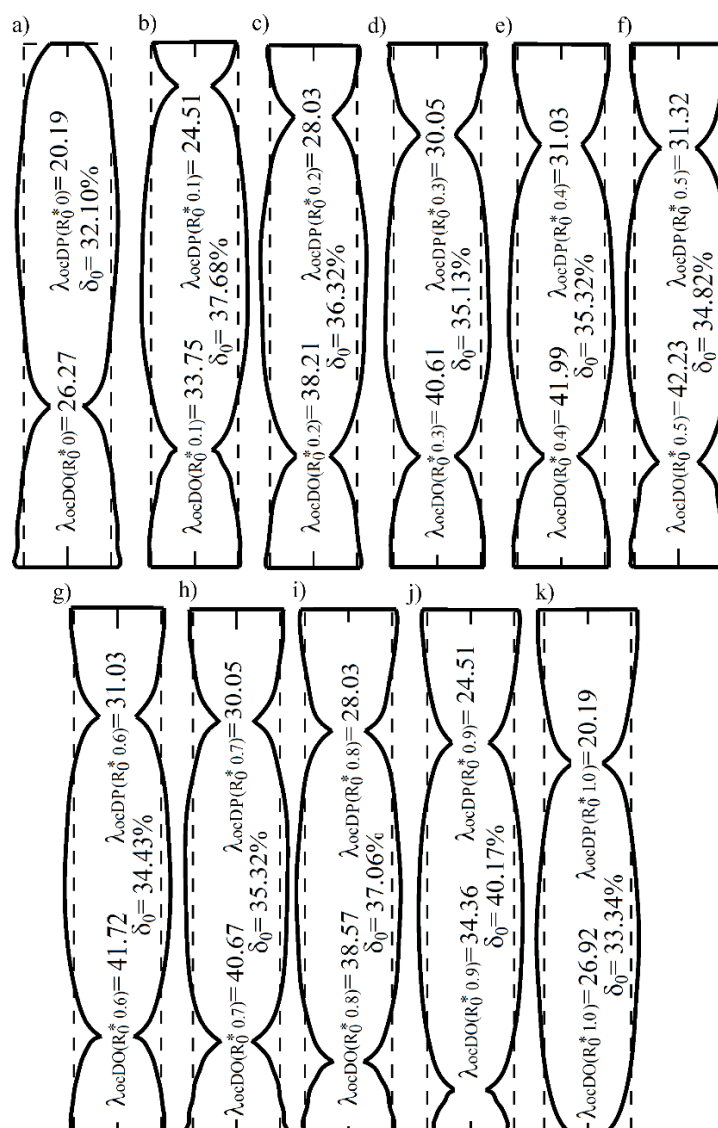


Figure 6 The shape of the optimized column $DO(R_o^*, j)$ with the variable parameter value R_o^*, j of the loading and load taking head: a) $R_o^* = 0$, b) $R_o^* = 0.1$, c) $R_o^* = 0.2$, d) $R_o^* = 0.3$, e) $R_o^* = 0.4$, f) $R_o^* = 0.5$, g) $R_o^* = 0.6$, h) $R_o^* = 0.7$, i) $R_o^* = 0.8$, j) $R_o^* = 0.9$, k) $R_o^* = 1.0$

corresponding optimized and prismatic column, as well as the percentage increase of the critical load parameter, were given. It has been limited to the selected values of the parameter R_o^* of the loading and load taking head. In a specific case $R_o^* = 0$ (Figure 6a), a characteristic feature for all the presented shapes is the presence of narrowings in the cross-section along the length of the columns. The location of the points described by the minimum value of the diameter depends on the value of geometric parameters of heads that are involved in the specific load case discussed.

8.2 Results of numerical calculations - free vibrations

Taking into account the solution of the boundary issue, which has been obtained based on the kinetic stability criterion, numerical calculations were carried

out with regard to the value of natural vibrations frequency ω of a column $DO(R_o^*, j)$. Taking into account the variable flexural rigidity of optimized columns, it has been limited to determination of the nature of changes in the first two basic natural vibrations frequencies in a dimensionless form $(\Omega_{o1}, \Omega_{o2})$, as a function of a dimensionless load parameter λ_o , with selected values R_o^* , Δr of heads performing the specific load cases, which are discussed. The following is assumed:

$$\lambda_o = \frac{PL^2}{(EJ)_p}, \quad (45)$$

$$\Omega_o = \frac{(\rho A)_p \omega^2 L^4}{(EJ)_p}, \quad (46)$$

where: A - cross-section area of the comparative column $(\rho A)_p$ - specific mass per unit length of the comparative column.

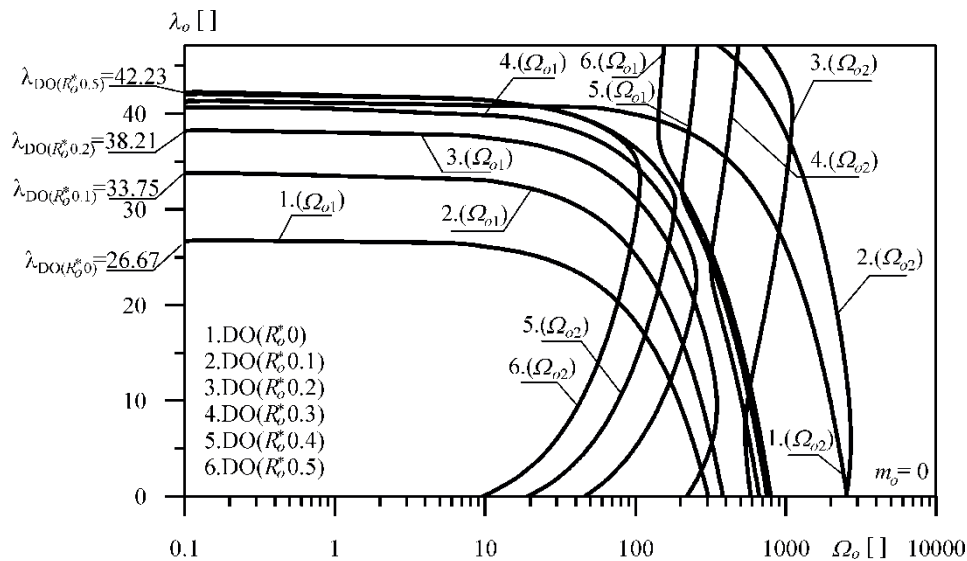


Figure 7 Curves on the plane load parameter λ_o - parameter of natural vibrations frequency λ_o (system $DO(R_o^*, j)$)

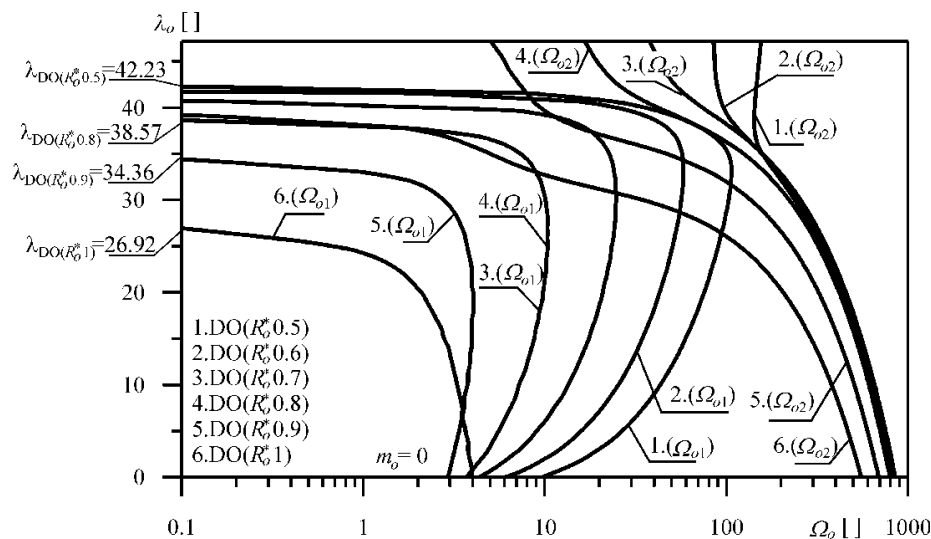


Figure 8 Curves on the plane load parameter λ_o - parameter of natural vibrations frequency λ_o (system $DO(R_o^*, j)$)

The results of numerical calculations of changes in eigenvalues of the column $DO(R_o^*, j)$ are presented in Figures 7 and 8. In case of $R_o^* = 0$ (the curves 1 - Figure 7), the scope of changes in the natural vibrations frequency corresponds to the model of the column in which the Euler load case was implemented.

The scope of changes of the basic natural vibrations frequency of columns $DO(R_o^*, j)$ and $DP(R_o^*, j)$, with selected parameters of heads R_o^* is shown in Figure 9. In the calculations, the zero value of the point mass m at the free end of the column was assumed, where:

$$m_o = \frac{m}{(\rho A)_p L}, \quad (47)$$

The value of the critical load of the discussed columns, in case of certain geometrical parameters of loading heads, were achieved with the parameter $\Omega_{o1} = 0$. The values of the critical load parameter, which were obtained based on the kinetic stability criterion,

are identical as in the case of application of the static criterion. Depending on the value of geometric parameters of the loading and load taking head, the presented courses of the basic frequency of natural vibrations Ω_{o1} , in the plane $\lambda_o - \Omega_o$ (Figure 9) have a negative, positive or zero inclination.

Figure 10 shows the forms of vibrations (M1, M2, M3) corresponding to the first three natural vibrations frequencies (parameters: Ω_{o1} , Ω_{o2} , Ω_{o3}) of the considered column. The forms of vibrations were determined with the normalization condition, assuming the value of the integrated constant of the motion equation result - normalization as to the constant, that is:

$$C_{ln} = 1 \quad (48)$$

Taking into account Equation (48) in the dependence in Equation (36), after the prior rejecting of one of the geometric boundary conditions, a heterogenous system

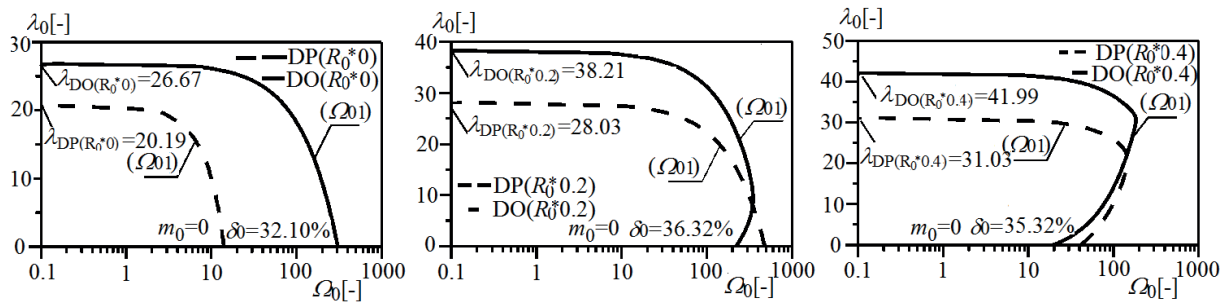


Figure 9 Curves on the plane load parameter λ_0 - basic frequency of natural vibrations parameter λ_{o1} of the optimized column $DO(R_0^* j)$ and the comparative column $DP(R_0^* j)$











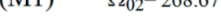


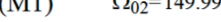




		DO ($R_0^*0.5$) column		
		Vibration form (M1, M2)		Vibration form (M3)
Load	$\lambda_0=1.88$	(M1)  $\Omega_{01}=16.04$	(M2)  $\Omega_{02}=760.3$	 $\Omega_{03}=4761.49$
	$\lambda_0=9.43$	(M1)  $\Omega_{01}=41.42$	(M2)  $\Omega_{02}=620.56$	 $\Omega_{03}=4210.04$
	$\lambda_0=16.98$	(M1)  $\Omega_{01}=66.03$	(M2)  $\Omega_{02}=479.67$	 $\Omega_{03}=3652.40$
	$\lambda_0=28.30$	(M2)  $\Omega_{01}=99.1$	(M1)  $\Omega_{02}=268.67$	 $\Omega_{03}=2801.76$
	$\lambda_0=35.84$	(M2)  $\Omega_{01}=96.81$	(M1)  $\Omega_{02}=149.99$	 $\Omega_{03}=2223.84$
	$\lambda_0=39.61$	(M2)  $\Omega_{01}=42.32$	(M1)  $\Omega_{02}=142.71$	 $\Omega_{03}=1931.29$

Figure 10 The forms of vibrations of the column $DO(R_0^* 0.5)$

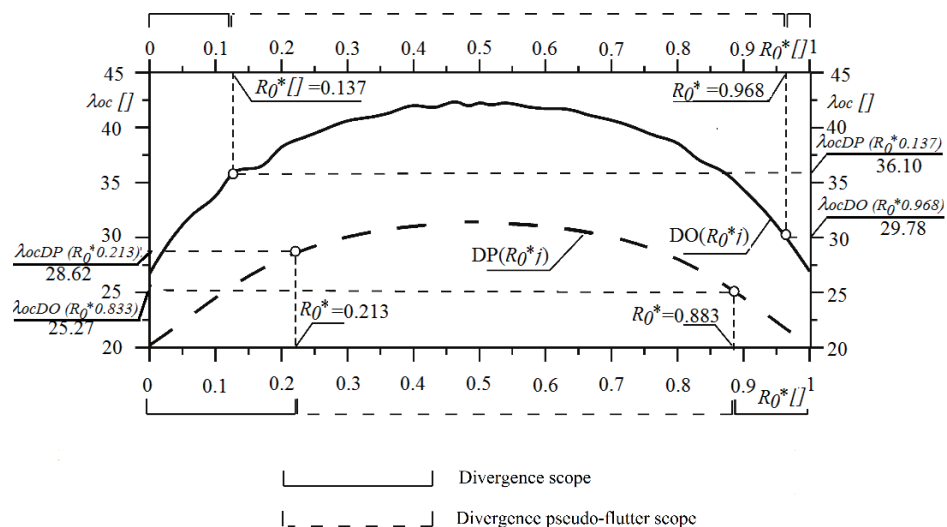


Figure 11 Divergence and divergence-pseudo-flutter scope of columns $DO(R_0^* j)$, $DP(R_0^* j)$

Table 1 Geometric and physical parameters of the column $DO(R_o^* j)$

E [Pa]	ρ [kg/m ³]	L [m]	b [m]	R [m]	l_0 [m]	m [m]
$7.5 \cdot 10^{10}$	2790	0.6	0.008	0.059	0.051	0.39

of equations with $(n-1)$ unknowns $C\kappa_i$ ($i=1, \dots, n$, $\kappa=1, \dots, 4$) was obtained. Based on the result of the system of equations, the remaining integration constants $C\kappa_i$ were determined. The forms of vibrations of the columns, with the natural vibrations frequency parameters $\Omega_o \zeta$ ($\zeta = 1, 2, \dots$) were described with relations in Equation (34). The scope of changes in the forms of natural vibrations is presented (Figure 10) as a function of external load regarding the selected geometry of the loading and load taking head ($R_o^* = 0.5$).

In a general case ($M\zeta$), the form of vibrations corresponding to ζ - of this frequency of natural vibrations ($\zeta = 1, 2, \dots$) has $(\zeta-1)$ nodes.

Based on numerical calculations, a change in the forms of vibrations ((M1), (M2)) was observed on the curves of the first and second natural vibrations frequency. In the case of the comparative column $DO(R_o^* j)$, this phenomenon was confirmed by experimental studies using the modal analysis.

The obtained nature of changes in eigenvalues (see Figure 7 to 9) and the scope of changes of the forms of natural vibrations along the curve $\lambda_o = f(\Omega_o)$ (see Figure 10), allows to include the optimized and comparative columns, subjected to a specific load, to one of two types of systems: divergent ($(d\Omega_{o1}/d\lambda_o)|_{\lambda_{o=0}} < 0$) or divergent - pseudo-flattery ($(d\Omega_{o1}/d\lambda_o)|_{\lambda_{o=0}} > 0$). Figure 11 presents the scope of changes in the value of the parameter R_o^* of the head taking the load with the force directed towards the pole, where the optimized column $DO(R_o^* j)$ and the comparative column $DP(R_o^* j)$ are included to one of two above-mentioned types of systems.

8.3 Experimental studies

This section of the paper presents the results of experimental studies and numerical calculations of the optimized system with the selected geometry of the head taking the load with follower force directed towards the positive pole $DO(R_o^* j)$. The physical and geometric parameters of the analyzed column are given in Table 1.

A rectangular cross-section of the analyzed column of dimensions a and b , was assumed for the calculations and experimental studies. Taking into account the criterion of the constant volume of the system; the width of the cross-section a was assumed (a_i - decision variables of the optimization process) with its fixed thickness b . In the applied modified method of simulated annealing, an additional condition was included in the following form:

$$a \geq b + 0.001 \text{ [m]} \quad i = 1, \dots, n. \quad (49)$$

Geometric inequality constraint in Equation (49) of the optimized column is justified due to the buckling plane of the system assumed in the numerical calculations and experimental systems, described with the minimum moment of inertia with respect to the neutral axis in the bending plane.

An experimental study was carried out at the stand, which was designed and constructed in the Department of Mechanics and Machine Design of the Czestochowa University of Technology. The stand (Figure 12) is composed of a support frame (1) to which the head (2) is attached. The element of the head (2) consists of a screw system by means of which the force loading the analyzed column (5) was generated with the use of a dynamometer (3) and a plate (4). Supports were attached to plates 8(1) and 8(2), which were implementing the required boundary conditions of the column. With four ball bearings (6), used at the pivots of the plate (4), a rectilinear shift was ensured in the guides (7). The guides (7) were attached to plate 8(1). The loading head (9), which was implementing the required boundary conditions at the free end of the analyzed system, was attached to the plate (4). The conditions of rigid bracing of the column is ensured by the element (1), which was attached to plate 8(2) with the housing (11). The head taking the load (12) was attached to the analyzed column with the use of block (13). It is assumed that the components:

- of the loading head (6),
- of the head taking the load to the column (12), (13), are infinitely rigid. It is justified due to construction purposes. Figure 12 also presents the diagram of the measurement system. The measurement system consists of a modal hammer (15) (Brüel&Kjaer type 8200 + 2646), a laser vibrometer (14) (VH - 1000 - D made by OMETRON), an analyzer (17) (Brüel&Kjaer type 3560C) and a computer (18) with the software PULSE (version 7.0). The modal hammer is connected to the analyzer only when the experimental modal analysis is performed.

As a part of numerical calculations, with a static stability criterion, the shape of the optimized column was determined. Taking into account the rigid elements in Equations (12), (13) of the load taking head (see Figure 12) in the mathematical model of the system, the boundary conditions (11) and (15) at the free end of the column ($x_n = l$) are modified. Thus, the following is obtained:

$$\begin{cases} W_n(l, t) - (R - l_0) \frac{\partial W_n(x_n, t)}{\partial x_n} \Big|_{x_n=l} = 0, \\ \frac{\partial^3 W_n(x_n, t)}{\partial x_n^3} \Big|_{x_n=l} - \frac{1}{(R - l_0)} \frac{\partial^2 W_n(x_n, t)}{\partial x_n^2} \Big|_{x_n=l} - \\ - \frac{m}{(EJ_n)} \frac{\partial^2 W_n(x_n, t)}{\partial t^2} = 0 \end{cases} \quad (50)$$

where l_0 - total length of rigid elements in Equation (12) and Equation (13) - see Figure 12.

The shape of the optimized column $DO(R_o^* 0.0125)$ (solid lines), obtained based on the solution of the

boundary issue, with the use of modified boundary conditions in Equation (50) is shown in Figure 14. The dashed line presents an outline of a relevant comparative column $DP(R_o^* 0.0125)$. In the case of the optimized shape of the system obtained, the critical load increase by 24.3% was achieved. The structural solutions of the research stand presented in Figure 12 are also shown in the picture (Figure 13b). In the pictures (Figures 13a and 13c) the shape of the examined column and the design solution of the load taking head are presented, as well.

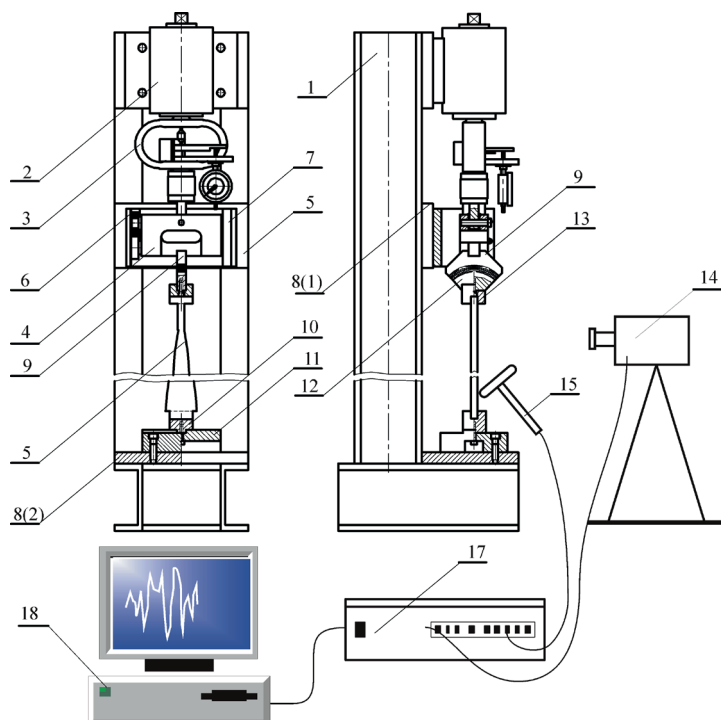


Figure 12 The stand for testing the natural vibrations of columns located in a vertical position

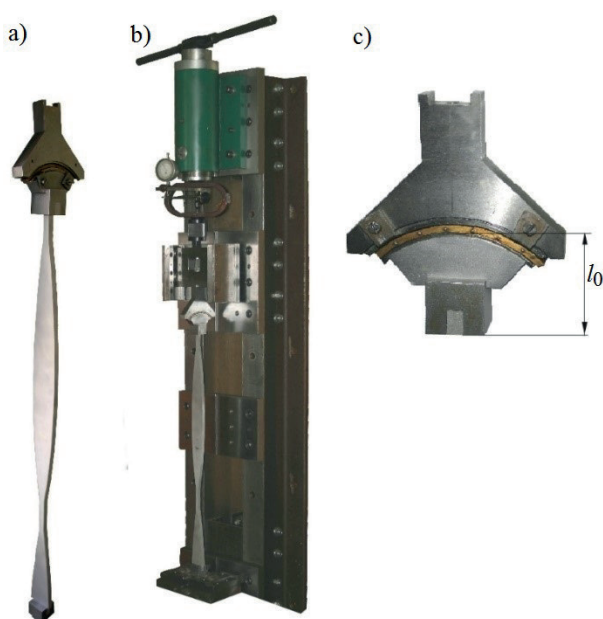


Figure 13 a) shape of the examined column b) stand for examining vibrations of the slender systems with a mounted column, c) load taking head

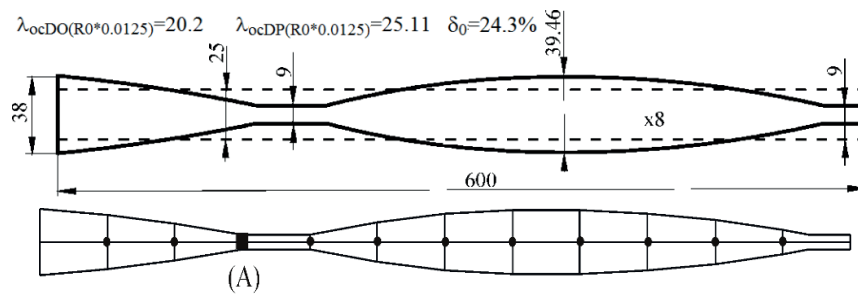


Figure 14 Shapes of columns: $DO(R_0^* 0.0125)$, $DP(R_0^* 0.0125)$. Model of the optimized column developed for the experimental modal analysis (the system $DO(R_0^* 0.0125)$)

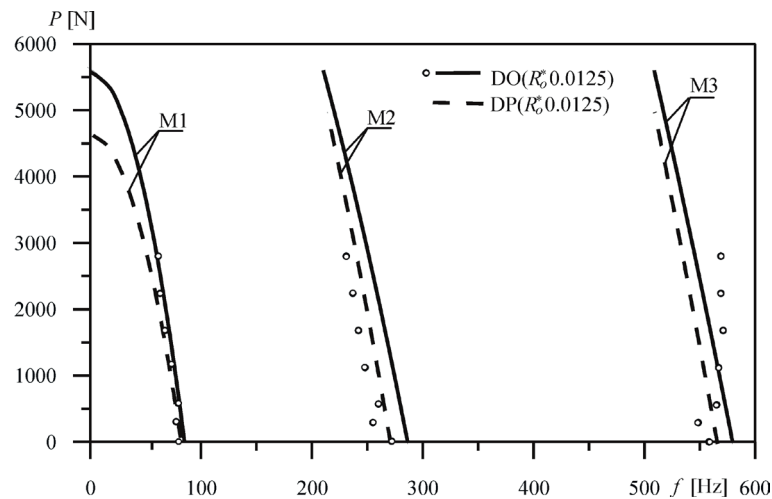


Figure 15 Curves on the plane load P - natural vibrations frequency f (the system $DO(R_0^* 0.0125)$)

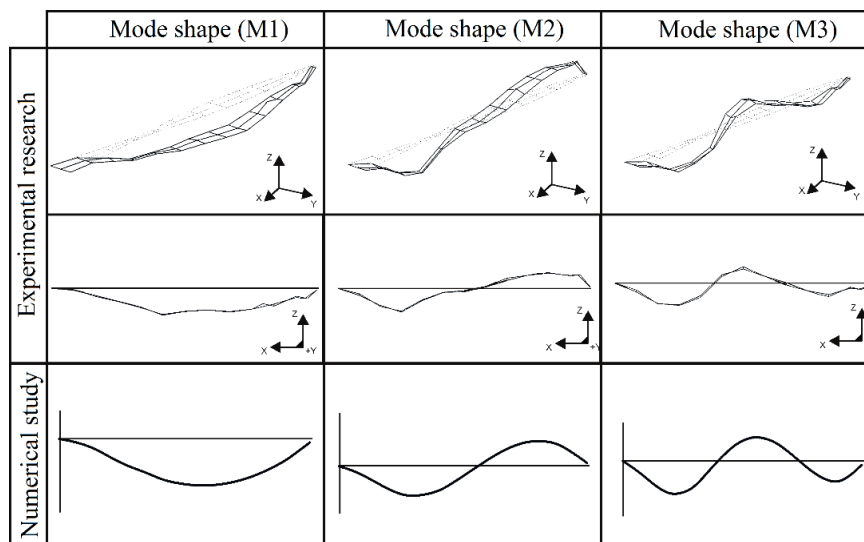


Figure 16 The forms of vibrations of the column $DO(R_0^* 0.0125)$ obtained based on the numerical calculations and experimental studies

Taking into account the obtained shape of the optimized column (Figure 14), experimental research was carried out with regard to changes in the frequency of natural vibrations and the form of natural vibrations of the considered system. For this purpose, experimental modal analysis was performed using the professional equipment and software.

Figure 14 presents also a non-deformed form of the examined system. Ten nodes, in which the measurements, were made were distinguished within the research object constructed with the use of PULSE 7.0 software. The forcing is realized by hitting the successive points (●) of the examined column with a modal hammer and simultaneously the velocity of displacement of the node

(A) of the column is measured with the use of a laser vibrometer. The signal from the modal hammer and laser vibrometer is sent to the analyzer and then to the computer using the ME'scopeVES 4.0 software from Vibrat Technology; the values of natural vibrations frequencies and the forms of natural vibrations of the optimized system were obtained. The results of numerical calculations (solid lines - the system $DO(R_o^* 0.0125)$) and experimental studies (points), regarding the changes in the frequencies of natural vibrations, are presented in Figure 15.

The dashed lines show the course of changes in the eigenvalues of the comparative column $DP(R_o^* 0.0125)$. The scope of changes of the first three frequencies of natural vibrations f , as a function of external load P was given. Comparing the results of numerical calculations and experimental studies of the column $DO(R_o^* 0.0125)$, a good consistency of the results was found. The maximum relative error with the basic natural vibrations frequency, between the experimental results f^e and the frequencies obtained in theory f^t , was 7.24%.

The forms of the transverse natural vibrations of the column (M1, M2, M3), obtained during the experiments and thanks to numerical calculations, are shown in Figure 16. The relevant results were shown with the external load value $P = 1640$ [N] and the geometric and physical parameters of the system from Table 1.

9 Conclusions

In this work, the issues of stability and natural vibrations of slender elastic systems modelling the bridge span subjected to the follower force directed to the positive pole were analyzed and examined. Based on the principle of minimum potential energy, displacement equations and boundary conditions were determined. Considering the variable flexural stiffness of the systems, the leap equation was derived for the critical load value - the objective function of the optimization problem. The simulated annealing algorithm was used in the considerations. The values of the critical load parameter of columns, optimized for the adopted criterion of constant volume of systems, were obtained. An increase in the critical load of optimized columns of 40.64% was obtained. It was found that there are such values of the head carrying the load parameters, at which the maximum value of the critical load parameter

is obtained. The obtained shapes of optimized columns are characterized by the occurrence of the cross-section narrowing points along the length of the columns. The location of these points depends on the value of the geometrical parameters of the heads carrying the load. Based on the results of numerical calculations, it should be stated that the simulated annealing algorithm is an effective method of searching for the extreme of functions of many variables and can be used to optimize the shape of slender systems. Modifications proposed in the work, the adopted calculation method (modified algorithm of simulated annealing), were aimed at accelerating the process of searching for the optimal solution.

In the field of dynamics of systems (vibration method), based on the Hamilton's principle and total mechanical energy of systems, the corresponding equations for motion equations and boundary conditions were derived within the scope of loss of the rectilinear form of equilibrium. Solving the boundary problem enabled numerical calculations to determine the range of changes in the frequency of vibrations as a function of the load of optimized columns. Diagrams of eigenvalues on the plane were obtained: load parameter λ_o - eigenfrequency parameter Ω_o and eigen vibration forms. It has been shown that the critical load values obtained based on the kinetic stability criterion are the same when applying the static criterion. The correctness of the adopted mathematical model of the system was confirmed by presenting the results of experimental research. Discussing the impact of external load and geometrical parameters of the heads: forcing and taking over the load on the nature of changes in the frequency of natural vibrations, including the corresponding forms of vibrations, the considered systems were classified as divergent or divergent pseudoflatter type systems.

Grants and funding

The authors received no financial support for the research, authorship and/or publication of this article.

Conflicts of interest

The authors declare that they have no known competing financial interests or personal relationships that could have appeared to influence the work reported in this paper.

References

- [1] UZNY, S., SOKOL, K. Critical load of a differently mounted columns determined according to the Bernoulli-Euler and Timoshenko theories. *Machine Dynamics Research*. 2015, **39**(2), p. 5-14. ISSN 2080-9948.
- [2] TOMSKI, L., UZNY, S. A hydraulic cylinder subjected to Euler's load in aspect of the stability and free vibrations taking into account discrete elastic elements. *Archives of Civil and Mechanical Engineering*

- [online]. 2011, **XI** (3), p. 769-785. ISSN 1644-9665. Available from: [https://doi.org/10.1016/S1644-9665\(12\)60115-0](https://doi.org/10.1016/S1644-9665(12)60115-0)
- [3] PRZYBYLSKI, J., SOKOL, K. Shape control of an eccentrically loaded column by means of a piezoceramic rod. *Thin - Walled Structures* [online]. 2011, **49**(5), p. 652-659. ISSN 0263-8231, eISSN 1879-3223. Available from: <https://doi.org/10.1016/j.tws.2010.09.014>
- [4] SZMIDLA, J., JURCZYNSKA, A. Stability of geometrically nonlinear pre-stressed column loaded by a force directed towards the positive pole partially lying on winkler elastic foundation. In: International Conference on Numerical Analysis and Applied Mathematics 2014 ICNAAM-2014: proceedings. AIP. 2014. ISBN 978-0-7354-1287-3, ISSN 0094-243X.
- [5] COLMENARES, D., ANDERSSON, A., KAROUMI, R. Closed-form solution for mode superposition analysis of continuous beams on flexible supports under moving harmonic loads. *Journal of Sound and Vibration* [online]. 2021, **520**, 116587. ISSN 0022-460X, eISSN 1095-8568. Available from: <https://doi.org/10.1016/j.jsv.2021.116587>
- [6] APSEMETOV, M., MADANBEKOV, N., MUKTAROV, T. Determination of the own forms of vibration of the span of beam bridges on elastic supporting parts. *E3S Web of Conferences* [online]. 2021, **263**, 02018. eISSN 2267-1242. Available from: <https://doi.org/10.1051/e3sconf/202126302018>
- [7] RUILAN, T., XINWEI, Y., ZHANG, Q., XIUYING, G. Vibration reduction in beam bridge under moving loads using nonlinear smooth and discontinuous oscillator. *Advances in Mechanical Engineering* [online]. 2020, **8**(6), p. 1-12. ISSN 1687-8132, eISSN 1687-8140. Available from: <https://doi.org/10.1177/168781401665256>
- [8] WAGG, D., NEILD, S. *Nonlinear vibration with control for flexible and adaptive structures. Chapt. 1: Introduction to nonlinear vibration and control, serial solid mechanics and its applications* [online]. Vol. 218. Switzerland: Springer International Publishing, 2015. ISBN 978-90-481-2836-5, p. 1-35. Available from: <https://doi.org/10.1007/978-90-481-2837-2>
- [9] AKOUR, S. N. Parametric study of nonlinear beam vibration resting on linear elastic foundation. *Journal of Mechanical Engineering and Automation* [online]. 2012, **2**(6), p. 114-134. ISSN 2163-2405, eISSN 2163-2413. Available from: <https://doi.org/10.5923/j.jmea.20120206.02>
- [10] GIZEJOWSKI, M. A., SZCZERBA, J., GAJEWSKI, M. D., STACHURA, Z. Buckling resistance assessment of steel I-section beam-columns not susceptible to LT-buckling. *Archives of Civil and Mechanical Engineering* [online]. 2017, **17**, p. 205-221. ISSN 1644-9665. Available from: <https://doi.org/10.1016/j.acme.2016.09.003>
- [11] SZMIDLA, J., JURCZYNSKA, A. Local loss of a rectilinear form of a static equilibrium of geometrically nonlinear system with non-prismatic element under force directed towards the pole. *Acta Physica Polonica A* [online]. 2020, **138**(2), p. 140-143. ISSN 1898-794X. Available from: <https://doi.org/10.12693/APhysPolA.138.140>
- [12] YAGHOUBI, H., TORABI, M. An analytical approach to large amplitude vibration and post-buckling of functionally graded beams rest on non-linear elastic foundation. *Journal of Theoretical and Applied Mechanics*. 2013, **51** (1), p. 39-52. ISSN 1429-2955.
- [13] ELMAGUIRI, M. N., HATERBOUCH, M., BOUAYAD, A., OUSSOUADDI, O. Geometrically nonlinear free vibration of functionally graded beams. *Journal of Materials and Environmental Science*. 2015, **6**(12), p. 3620-3633. ISSN 2028-2508.
- [14] KUMAR, S., MITRA, A., ROY, H. Geometrically nonlinear free vibration analysis of axially functionally graded taper beams. *An International Journal of Engineering Science and Technology* [online]. 2015, **18**(4), p. 579-593. eISSN 2215-0986. Available from: <https://doi.org/10.1016/j.jestch.2015.04.003>
- [15] SZMIDLA, J., WAWSZCZAK, A. Optimization of the shape of columns implementing selected cases of Euler load using a modified algorithm of simulated annealing a (in Polish). In: 13th Structural Dynamics Symposium DYNKON 2008: proceedings. Vol. 258, Mechanics series74. p. 333-344.
- [16] NIKOLIC, A., SALINIC, S. Buckling analysis of non-prismatic columns: a rigid multibody approach. *Engineering Structures* [online]. 2017, **143**, p. 511-521. ISSN 0141-0296, eISSN 1873-7323. Available from: <https://doi.org/10.1016/j.engstruct.2017.04.033>
- [17] SZMIDLA, J., JURCZYNSKA, A. The tapered column shape optimisation in a plane perpendicular to the buckling plane subjected to a load by the follower force directed to the positive pole. *Machine Dynamics Research*. 2015, **39**(2), p. 33-44. ISSN 2080-9948.
- [18] ZHOU, G., QIAN, C., CHEN, C. Research on the approximate calculation method of the fundamental frequency and its characteristics a tensioned string bridge. *Processes* [online]. 2022, **10**, 126. eISSN 2227-9717. Available from: <https://doi.org/10.3390/pr10010126>
- [19] GARINEI, A. Vibrations of simple beam-like modelled bridge under harmonic moving loads. *International Journal of Engineering Science* [online]. 2006, **44**(11-12), p. 778-787. ISSN 0020-7225, eISSN 1879-2197. Available from: <https://doi.org/10.1016/j.ijengsci.2006.04.013>

- [20] RASPOPOV, A., ARTYOMOV, V., RUSU, S. The simulation of vibrations of railway beam bridges in the object-oriented environment Delphi. *The Archives of Transport* [online]. 2010, **XXII**(4), p. 463-476. ISSN 0866-9546. Available from: <https://doi.org/10.2478/v10174-010-0028-8>
- [21] ZANGENEH, A., MUSEROS, P., PACOSTE, C., KAROUMI, R. Free vibration of viscoelastically supported beam bridges under moving loads: closed-form equation for maximum resonant response. *Engineering Structures* [online]. 2021, **244**, 112759. ISSN 0141-0296, eISSN 1873-7323. Available from: <https://doi.org/10.1016/j.engstruct.2021.112759>
- [22] KOPIIKA, N., VEGERA, P., VASHKEVYCH, R., BLIKHARSKYY, Z. Stress-strain state of damaged reinforced concrete bended elements at operational load level. *Production Engineering Archives* [online]. eISSN 2353-7779. 2021, **27**(4), p. 242-247.
- [23] DOUNGPORN, W., NATHNARONG, K., YONG, H. W. Effect of beam joinery on bridge structural stability. *Advances in Difference Equations* [online]. 2019, **2019**, 225. eISSN 2731-4235. Available from: <https://doi.org/10.1186/s13662-019-2158-5>
- [24] LI, Q. S. Exact solutions for buckling of non-uniform columns under axial concentrated and distributed loading. *European Journal of Mechanics - A/Solids* [online]. 2001, **20**(3), p. 485-500. ISSN 0997-7538, eISSN 1873-7285. Available from: [https://doi.org/10.1016/S0997-7538\(01\)01143-3](https://doi.org/10.1016/S0997-7538(01)01143-3)
- [25] LI, Q. S. Stability of non-uniform columns under the combined action of concentrated follower forces and variably distributed loads. *Journal of Constructional Steel Research* [online]. 2008, **64**(3), p. 367-376. ISSN 0143-974X, eISSN 1873-5983. Available from: <https://doi.org/10.1016/j.jcsr.2007.07.006>
- [26] SERNA, M. A., IBANEZ, J. R., LOPEZ, A. Elastic flexural buckling of non-uniform members: closed-form expression and equivalent load approach. *Journal of Constructional Steel Research* [online]. 2011, **67**(7), p. 1078-1085. ISSN 1873-5983, eISSN 0143-974X. Available from: <https://doi.org/10.1016/j.jcsr.2011.01.003>